

## Iron, manganese and aluminium oxides and oxyhydroxides

VIDAL BARRÓN\* and JOSÉ TORRENT

*Departamento de Agronomía, Universidad de Córdoba, Edificio C4,  
Campus de Rabanales, 14071 Córdoba, Spain*

*\*e-mail: vidal@uco.es*

Nanosized iron, manganese and aluminium oxides are abundant in soils and sediments, but are also present in water and air, and are even produced within living organisms. These minerals play major roles in the biogeochemical cycles of Fe, Mn and Al; the adsorption and transport of ions, including nutrients and toxic metals; and redox processes. They also influence the physical properties and erodibility of soils. This chapter reviews some aspects of their formation pathways and occurrence in natural environments, and discusses their crystal structure, morphology and size in relation to the nanoscale reactions in which they take part.

### 1. Introduction

Iron (Fe), manganese (Mn) and aluminium (Al) oxides (a term used here to refer to hydroxides and oxyhydroxides also), together with phyllosilicate clay minerals, are the most abundant nanominerals and mineral nanoparticles in many natural environments, especially soils. As part of the critical zone of the Earth, soils are the interface where the lithosphere meets with the hydrosphere, biosphere and atmosphere. They provide us with food, fibre and many other natural resources. The Fe, Mn and Al oxides in soils are typically nanosized and possess large surface areas compared to other soil minerals such as quartz or feldspars, which are typically one to three orders of magnitude more abundant and greater in particle size. These properties are the keys to their roles in elemental biogeochemical cycles involving various phenomena such as the adsorption and transport of ions (nutrients and toxic metals/molecules included), redox processes affecting Fe or Mn, and soil erodibility. It is therefore important to understand their formation pathways and occurrence in natural environments. This requires a sound knowledge not only of their original sources (soils, acid mine drainage, organisms), but also of the hydrospheric and atmospheric fluids that carry them around the Earth.

Our writing of this chapter was facilitated enormously by the vast information about Fe oxides compiled in the extraordinary book *The Iron Oxides: Structure, Properties, Reactions, Occurrence and Uses* by Cornell & Schwertmann (2003), which includes much of the research conducted by U. Schwertmann and coworkers from many countries. This *opus magnum* was supplemented with a recent review about naturally occurring Fe

oxide nanoparticles by Guo & Barnard (2013) and the summarized information contained in a book chapter by Bigham *et al.* (2002) which follows the classic 'Iron oxides' chapter in the second edition of *Minerals in Soil Environments* (Schwertmann & Taylor, 1989). The latter book also provides comprehensive reviews of the nature, formation and occurrence of Mn (McKenzie, 1989; Dixon & White, 2002) and Al oxides (Hsu, 1989; Huang *et al.*, 2002), and of their environmental significance.

Much research about the properties and reactivity of Fe oxides has been performed on synthetic samples, which have been used as model systems for better understanding of the complex phenomena occurring in natural environments. The book by Schwertmann & Cornell (2000), and the references therein, contain a number of recipes for "cooking" ultrafine Fe oxides of different morphologies and sizes. Additional methods, for example, for growing very small nano-hematite particles can be found in Madden & Hochella (2005) or Barton *et al.* (2012).

**Table 1.** Scientific papers published in journals listed by the Thomson Reuters' *Science Citation Index* from 1990 to May 2012.

	Total number of papers <sup>1</sup>	TEM or HRTEM or SEM <sup>2</sup>	STM or AFM <sup>3</sup>
<i>Iron oxides</i>			
Magnetite	16489	2358	247
Hematite	9304	1376	176
Goethite	6342	763	60
Maghemite	2161	491	41
Ferrihydrite	2500	362	21
Lepidocrocite	887	169	16
Akaganeite	381	100	3
Schwertmannite	365	54	0
Feroxyhyte	30	10	0
<i>Manganese oxides</i>			
Manganite	12060	641	124
Hollandite	540	86	0
Pyrolusite	355	39	3
Cryptomelane	360	94	2
Todorokite	258	69	1
Ramsdellite	185	19	1
Romanechite	38	2	1
Birnessite	944	181	10
Lithiophorite	70	10	1
Chalcophanite	26	0	0
<i>Aluminium oxides</i>			
Gibbsite	1943	219	31
Boehmite	2178	539	27
Diaspore	1082	49	8
Bayerite	297	54	3
Average ratio vs. total number of papers (%)		16	1

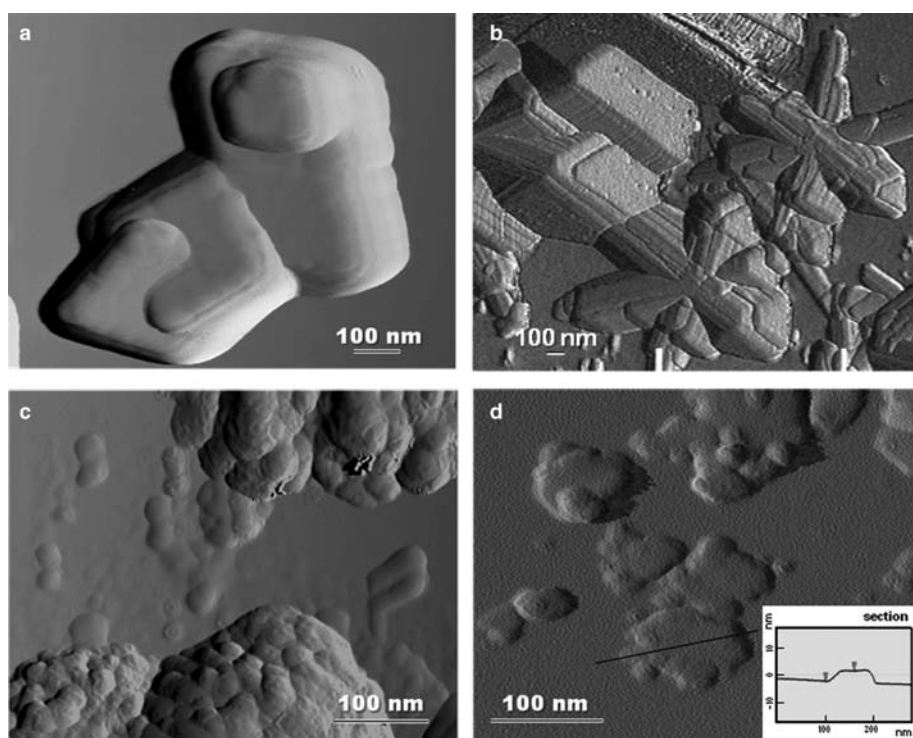
<sup>1</sup>Total cites before 1990 were <10%

<sup>2</sup>TEM (transmission electron microscopy), HRTEM (high-resolution transmission electron microscopy); SEM (scanning electron microscopy).

<sup>3</sup>STM (scanning tunnelling microscopy), AFM (atomic force microscopy)

As shown in many studies, proper study of nanosized Fe, Mn and Al oxides requires use of ‘nanoscale microscopy’ which we should perhaps refer to as ‘nanoscopy’. Based on the Science Citation Index database (checked in 2012), 16% of all papers dealing with oxides since 1990 mention explicitly, in the title, abstract or keywords, the use of transmission electron microscopy (TEM), high resolution transmission electron microscopy (HRTEM) or scanning electron microscopy (SEM) for the characterization of these minerals, especially in the nanoscale range (Table 1). Below we describe a number of examples where the multiple sizes and shapes made ‘visible’ by these techniques have been crucial to explaining the behaviour of the different types of oxides.

Scanning tunnelling microscopy (STM) and atomic force microscopy (AFM) have proved successful in other fields of nanotechnology and reached atomic-level resolution. However, good observations are relatively scant, and exist only for relatively large particles of hematite, magnetite, corundum or some Mn oxides (Wang *et al.*, 1998; Lower *et al.*, 2001; Barth & Reichling, 2001; Weiss & Ranke, 2002; Renner *et al.*, 2002). Figure 1 shows some examples of serious problems, such as instrument artifacts or particle aggregation, which arose when Fe oxides nanoparticles were



**Fig. 1.** AFM images of synthetic iron oxides: (a) hematite; (b) goethite with instrumental pyramidal artifacts; (c) ferrihydrite, and (d) lepidocrocite; inset, a cross section representing the line marked on the particle.

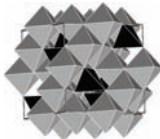

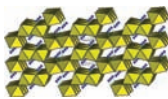
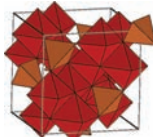
imaged by AFM. As a result, these techniques have been the subject of much fewer published studies than others based on electron microscopy (Table 1). Lastly, the large number of publications relating to Fe oxides relative to Mn and Al oxides calls for more attention to the Fe oxides.



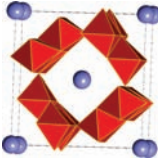
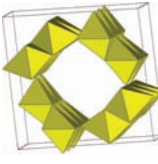

## 2. Iron oxides

### 2.1. Crystal structure, morphology and size

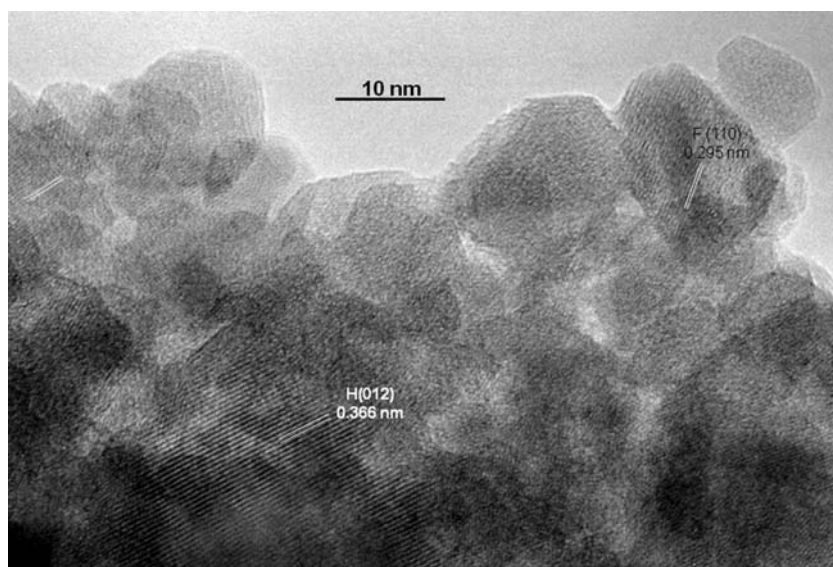
Accurate knowledge of the crystal structure, morphology and size of Fe oxides is crucial to understanding many of their properties including colour, solubility, adsorption capacity and surface reactions. Precise elucidation of the atomic structure of Fe oxides has been enabled by X-ray and neutron diffraction (either conventional or synchrotron radiation-based), ultraviolet-visible-infrared (UV-Vis-IR) and Mössbauer spectroscopies, and the microscopic techniques TEM, HRTEM and SEM. The crystallographic structures of the main crystalline Fe oxides are well known (Table 2; Cornell & Schwertmann, 2003). Nevertheless, it should be noted that, as shown by Banfield & Zhang (2001), Spagnoli *et al.* (2009) or Hiemstra (2013), surface structure, which is key in nanoparticle reactivity, is substantially different from bulk structure.

*Table 2.* Crystallographic data and structure for iron oxides.

Mineral	Formula	Crystal system	Unit-cell dimension (nm)			Structure
			<i>a</i>	<i>b</i>	<i>c</i>	
Magnetite	Fe <sub>3</sub> O <sub>4</sub>	Cubic	0.8396			
Hematite	α-Fe <sub>2</sub> O <sub>3</sub>	Trigonal	0.5034		1.3752	
Goethite	α-FeOOH	Orthorhombic	0.9956	0.3021	0.4608	
Maghemite	γ-Fe <sub>2</sub> O <sub>3</sub>	Cubic or tetragonal	0.8347		2.5010	

Ferrihydrite	$\text{Fe}_{10}\text{O}_{14}(\text{OH})_2 \cdot n\text{H}_2\text{O}$	Hexagonal	0.5902		0.9260	
Lepidocrocite	$\gamma\text{-FeOOH}$	Orthorhombic	0.3071	1.2520	0.3873	
Akaganeite	$\beta\text{-FeOOH Cl}$	Monoclinic	1.0560	0.3031	1.0840	
Schwertmannite	$\text{Fe}_8\text{O}_8(\text{OH})_6 \text{SO}_4$	Tetragonal	1.0660		0.6040	
Feroxyhyte	$\delta\text{-FeOOH}$	Hexagonal	0.2930		0.4560	

The structure of ferrihydrite is the subject of debate (Michel *et al.*, 2010; Barrón *et al.*, 2012; Manceau, 2012; and references therein). Michel, Barrón and co-workers (Michel *et al.*, 2010) advocate the presence of tetrahedrally coordinated iron(III) ( $\text{IVFe}$ ) in ferrihydrite, an assumption that is supported by several studies (Xu *et al.*, 2011; Mikutta, 2011; Harrington *et al.*, 2011; Maillot *et al.*, 2011; Derek & Tom, 2012; Guyodo *et al.*, 2012; Hiemstra, 2013) but contradicts the  $\text{IVFe}$ -free model (Drits *et al.*, 1993; Rancourt & Meunier, 2008; Hiemstra & Van Riemsdijk, 2009; Manceau, 2010, 2011, 2012). In that discussion some of the more cited papers are those of Janney *et al.* (2000a,b), which played a central role in the debate by performing a very careful study of 2- and 6-line ferrihydrite by HRTEM, selected-area electron diffraction, scanning transmission electron microscopy and nanodiffraction spectroscopy. Lattice fringes corresponding to an ordered ferrihydrite (110) plane (spacing of 0.29 nm) are shown in Figure 2 (Barrón *et al.*, 2003).



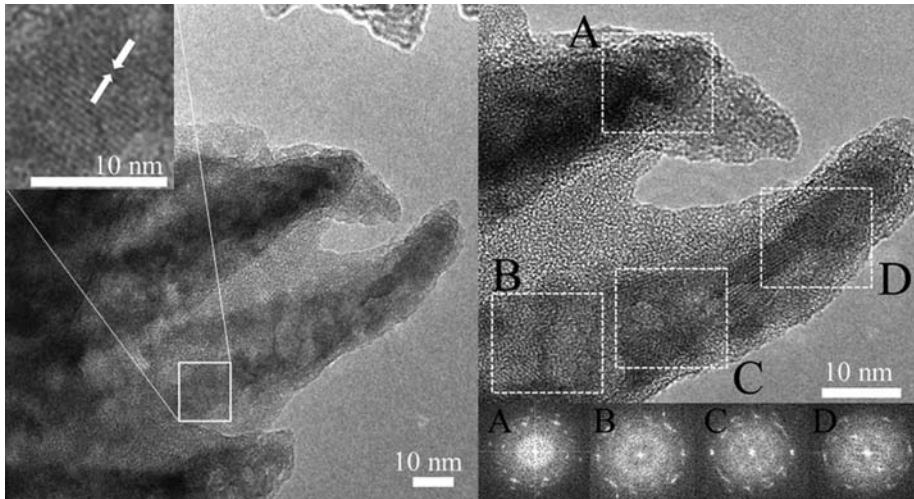
**Fig. 2.** TEM image with lattice fringes of ordered ferrihydrite (0.295 nm) mixed with hematite (0.366 nm) obtained by aging phosphated 2-line ferrihydrite (P/Fe 2.75%) at 150°C for 2 weeks.

There is also much discussion about the structure of the poorly crystalline schwertmannite (Fernández-Martínez *et al.*, 2010). Recently, French *et al.* (2012) suggested, on the basis of analytical HRTEM (Fig. 3), that this mineral should not be described as a single phase but as a polyphasic nanomineral with crystalline areas of goethite and jarosite (known transformation products of schwertmannite) within an amorphous matrix.

## **2.2. Formation of iron oxides: pathways and effect of temperature, pH, Eh and foreign compounds**

Iron is the fourth most abundant element in the Earth's crust, accounting for 5.1% of all elements (Clarke & Washington, 1924). It is a component of ferromagnesian silicates (olivine, pyroxenes, amphiboles, micas), Fe-Ti oxides (ilmenite, magnetite and titanomagnetite) and Fe sulfides, and is also present, in smaller proportions, in accessory silicates (*e.g.* tourmaline, epidote, garnet). Because these minerals crystallize from magmatic rocks under temperature and pressure conditions that are vastly different from those of the Earth's surface, they are unstable and easily weathered by exposure to atmospheric conditions. The transformation into Fe oxides can essentially take place *via* two different mechanisms, namely: (1) precipitation from Fe(II) or Fe(III) released by the effect of rock weathering; and (2) conversion of a precursor Fe oxide by dissolution/reprecipitation or *via* a solid-state process (Cornell & Schwertmann, 2003). The hydrolysis, oxidation, dehydration, dehydroxylation, redissolution and





**Fig. 3.** TEM images of needles on the surface of a schwertmannite particle from Rio Tinto mine (Spain). The inset in the image on the left shows lattice fringes (0.486 nm) assigned to goethite. The image on the right shows the tips of the needles with insets showing fast Fourier transform analysis of the lattice fringes where it was possible to distinguish spacing at 0.255, 0.228 nm (goethite) and 0.339 nm (jarosite) (reproduced from French *et al.*, 2012, with the permission of the Mineralogical Society of America).

crystallization reactions potentially involved make up a complex scenario (Fig. 4) where hematite ( $\alpha\text{-Fe}_2\text{O}_3$ ) and goethite ( $\alpha\text{-FeOOH}$ ) are the most common Fe oxides by virtue of their increased thermodynamic stability. The precursor of these minerals is very often ferrihydrite [ $\text{Fe}_{10}\text{O}_{14}(\text{OH})_2 \cdot n\text{H}_2\text{O}$ ], which can be converted to hematite by aggregation–dehydration–rearrangement or into goethite by dissolution–reprecipitation (Bigham *et al.*, 2002). Based on TEM data from Banfield *et al.* (2000) and Guyodo *et al.* (2003), goethite can also be self-assembled through aggregation and rotation of ferrihydrite nanoparticles adopting parallel orientations in the three dimensions. Other metastable phases such as ‘green rust’ [ $(\text{Fe}^{\text{III}}_x\text{Fe}^{\text{II}}_y(\text{OH})_{3x+2y-z}(\text{Cl}^-, \text{SO}_4^{2-}))$ ], magnetite ( $\text{Fe}_3\text{O}_4$ ), maghemite ( $\gamma\text{-Fe}_2\text{O}_3$ ), lepidocrocite ( $\gamma\text{-FeOOH}$ ), or schwertmannite [ $(\text{Fe}_8\text{O}_8(\text{OH})_6(\text{SO}_4) \cdot n\text{H}_2\text{O})$ ] can form *via* other pathways and even persist over pedogenic time scales. Environmental factors such as temperature, pH, redox potential, water activity, salts and/or foreign compounds, and the reaction time influence the proportions of the resulting phases. Factors such as soil pH, Eh, temperature and moisture regime also have an indirect effect on the nature and content of organic compounds that influence the previous formation pathways through complexation reactions.

Many of these factors govern the grain size and morphology of the resulting products (Schwertmann & Cornell, 2000; Cornell & Schwertmann, 2003; and references therein).

The extensive use of Fe oxides (especially magnetite and hematite) as catalysts has triggered considerable effort to find new ways to synthesize them as nanosized spheres, octahedra, cubes, pseudocubes, platelets, discs, stars, rods, wires, tubes,

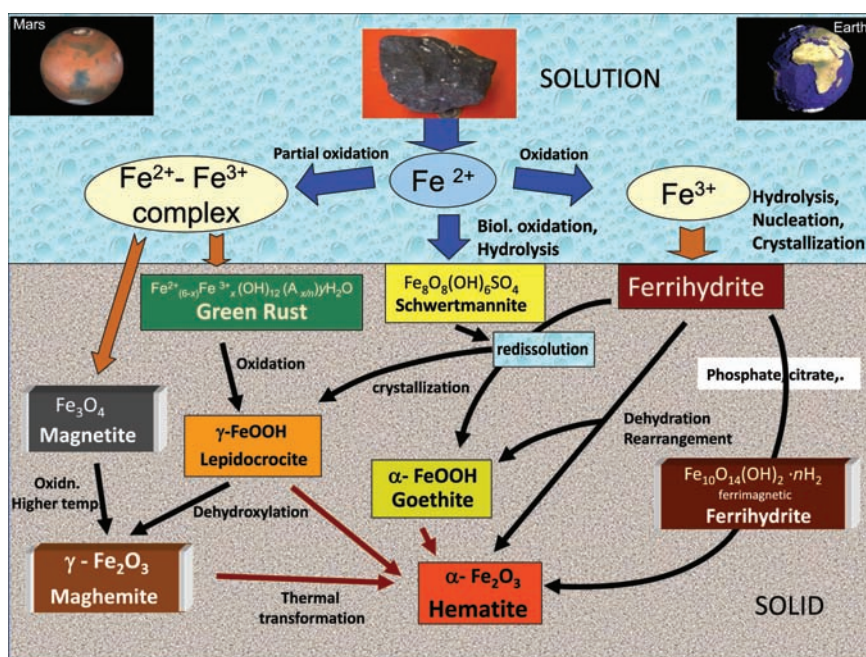


Fig. 4. Formation and transformation pathways for Fe oxides.

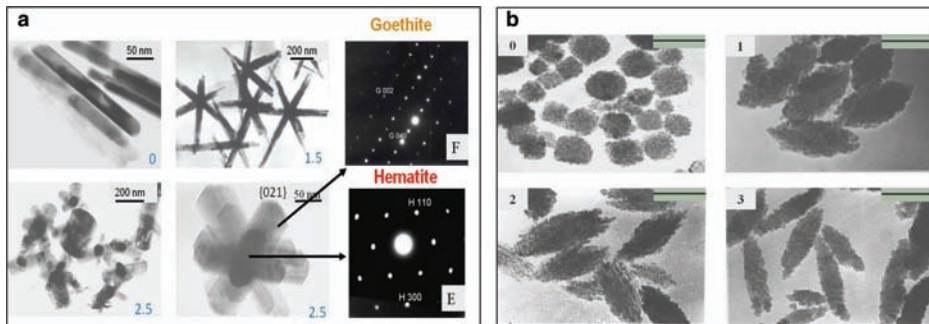
spindles, framboids, chains and tyre-, olive-, flower-, rice- and peanut-like particles (Ozaki *et al.*, 1984, 1990; Ocaña *et al.*, 1999; Mao *et al.*, 2007; Wang & Gao, 2010; Beveridge *et al.*, 2011; Huang *et al.*, 2011; Su *et al.*, 2011; Zhu *et al.*, 2011; Liu *et al.*, 2012; Wang *et al.*, 2012; Wheeler *et al.*, 2012; Guo *et al.*, 2013).

In order to mimic natural processes leading to the formation of Fe oxides, our research group has investigated the effect of pH, temperature and phosphate on the nature, shape and size of crystalline Fe oxides obtained by hydrothermal transformation of 2-line ferrihydrite (Barrón *et al.*, 1997; Gálvez *et al.*, 1999). Phosphate at atomic P/Fe ratios below 2.5% was found to strongly influence the morphology of the crystalline products, which were twinned goethite crystals with a hematite core (Fig. 5a) in alkaline media and spindle-shaped hematite crystals at acid to circumneutral pH values (Fig. 5b).

Crystallization of ferrihydrite was normally inhibited or delayed at  $P/Fe > 2.5\%$  by the effect of phosphate adsorbed on the ferrihydrite surface hindering aggregation prior to hematite formation. Under these conditions, temperatures  $>100^\circ\text{C}$  lead to the formation of an ordered ferrimagnetic ferrihydrite as an intermediate in the transformation into hematite (Barrón & Torrent, 2002; Barrón *et al.*, 2003; Michel *et al.*, 2010) (Fig. 2). Silicate, tartrate, citrate and other ligands can affect the crystallization of ferrihydrite at room temperature in a similar way as does phosphate (Cabello *et al.*, 2009).

Phosphate also plays a prominent role in the oxidation and transformation of Fe(II) salts by preventing the crystallization of goethite, the phase most commonly formed





**Fig. 5.** (a) TEM and electron diffraction images of iron oxides hydrothermally synthesized at 373 K, pH 12 and in the presence of phosphate in a P/Fe atomic ratio of 0, 1.5 or 2.5% (reproduced from Barrón *et al.*, 1997, with the permission of the Mineralogical Society of America); (b) TEM images of hydrothermally synthesized hematites at 373 K, pH 4, using a P/Fe atomic ratio of 0, 1, 2 or 3%. Bars represent 100 nm.

in its absence. Thus, Cumplido *et al.* (2000) obtained ferrihydrite or platy lepidocrocite with a large specific surface area and solubility at  $P/Fe > 2\%$ . This evidence provides a plausible explanation for the effectiveness of synthetic vivianite [ $Fe^{II}_3(PO_4)_2 \cdot H_2O$ ] in correcting Fe deficiency chlorosis in plants grown in calcareous soils (Roldán *et al.*, 2002; Rosado *et al.*, 2002). Thus, the incongruent dissolution of vivianite in an oxidized, alkaline soil medium resulted in the production of ferrihydrite and poorly crystalline lepidocrocite nanoparticles, the Fe of which was found to be plant available. Recent experiments involving the use of nanosiderite ( $FeCO_3$ ) to prevent Fe chlorosis point to the same mechanism, namely: the transformation of nanosiderite into poorly crystalline Fe oxides rather than into the more crystalline and poorly soluble goethite (Sánchez-Alcalá *et al.*, 2012a,b).

Also, Barrón *et al.* (2006) found that the presence of phosphate, significant ionic strength and acid conditions facilitated the incongruent dissolution of jarosite [ $(KFe^{III}_3(OH)_6(SO_4)_2)$ ] to a hematite nanophase, which might account for the jarosite-hematite paragenesis observed on the surface of Mars.

## 2.3. Occurrence in natural environments

### 2.3.1. Lithosphere and pedosphere

Iron oxides are widespread in rocks, sediments and soils, and are typically nanosized. Depending on the mineralogy of the parent rock and the maturity of the soil, the Fe oxides content ranges from  $<1$  to several hundred grams per kilogram. Iron present as Fe oxides is usually quantified by extraction with a strong reductant (typically sodium dithionite) (designated as  $Fe_d$ ; Mehra & Jackson, 1960) and comparison with the amount of total iron ( $Fe_t$ ) determined after digestion and dissolution of the soil or sediment, which includes Fe in primary minerals. Thus, the  $Fe_d/Fe_t$  ratio is an effective indicator of soil maturity (see the example chronosequences in Torrent, 1976, and Torrent *et al.*, 2010).

Together with magnetite, which is generally lithogenic, there are six pedogenic Fe(III) oxides, the global abundance of which decreases in the following sequence: goethite > hematite  $\geq$  ferrihydrite > maghemite > lepidocrocite > schwertmannite. Very often, two to four of these species coexist in soil. Table 3 summarizes the environmental conditions under which the different Fe oxide types are usually found in soils. Quantifying and characterizing soil Fe oxides requires the use of several complementary techniques including selective chemical dissolution, X-ray diffraction (XRD), electron microscopy, and thermal, magnetic or spectroscopic analysis. One widely used parameter in pedogenetic studies is the ratio of  $\text{NH}_4$ -oxalate extractable iron ( $\text{Fe}_{\text{ox}}$ ) which measures ferrihydrite-Fe mainly (Schwertmann, 1964), to  $\text{Fe}_{\text{d}}$ , which represents the total Fe oxides content. The topsoil contains organics that hinder crystallization of Fe oxides and usually exhibits the largest  $\text{Fe}_{\text{ox}}/\text{Fe}_{\text{d}}$  ratio in the soil profile as a result. Soils in humid and temperate regions have increased  $\text{Fe}_{\text{ox}}/\text{Fe}_{\text{d}}$  ratios relative to the more mature soils of tropical and subtropical regions, where crystalline goethite and hematite prevail (Cornell & Schwertmann, 2003).

Starting from the observations of the first astronomers several centuries ago, the colour of Mars was attributed to the potential presence of reddish Fe oxides. Although no samples from the Mars surface have yet been brought to the Earth, geochemical, magnetic and spectroscopic information derived from orbiters (Mariner), *in situ* landers (Viking), and rover missions (Pathfinder, Spirit, Opportunity, Phoenix) have

**Table 3.** Occurrence of different iron oxides in soils (Cornell & Schwertmann, 2003).

Mineral	Major soils
Goethite	Aerobic and anaerobic soils of all regions
Lepidocrocite	Anaerobic, Clayey, non-calcareous soils of cooler and temperate regions
Ferrihydrite	Groundwater and stagnant water soils (gleys and pseudogleys) and podsol of temperate and cool regions. Paddy soils.
Hematite	Aerobic soils of subtropical, Mediterranean and humid and subhumid tropical regions (lateritic and plinthic soils, red Mediterranean soils, oxisols, ultisols)
Maghemite	Aerobic soils of the tropics and subtropics. Soils with iron oxyhydroxide and organic matter after fire

enabled the identification of the Fe oxides present on the Mars surface (Chevrier & Mathé, 2007). Miniaturized instruments equipped with visible–infrared, Mössbauer and alpha particle X-ray spectroscopy, and magnetic measurements, or even an atomic force microscope to ‘visualize’ nanometric particles in the Phoenix mission, have extended available knowledge about the mineralogy of Mars and allowed its geological history to be ‘written’ (Pike *et al.*, 2011). Based on the classical model for the formation of Fe oxides (Fig. 4), sites where Fe oxides are present (especially as nanophase particles) constitute an aquamarker and hence a preferential location to search for extraterrestrial life (Squyres *et al.*, 2004). The new mission ‘Mars Rover Curiosity’, which is equipped with highly sophisticated instruments including a miniaturized X-ray diffractometer, is currently exploring the Martian surface and sending back further information on the mineralogy of that planet (<http://mars.jpl.nasa.gov/msl/>).

At present, there is scarce information about the mineralogy of the surface of another telluric inner planet: Venus. Data from landers (Venera and Vega) and theoretical models (*e.g.* one based on the surface temperature, which is estimated to be 750 K) have been used to predict that only hematite and magnetite are present on the surface of this planet (Fegley *et al.*, 1992).

### 2.3.2. Hydrosphere

Reddish- and yellowish-pigmented watercourses, or even unpleasantly pigmented domestic water, are not unusual and reflect the presence of particulate (mostly nanometric) Fe oxides, whether alone or associated with silicate clays or other mineral or organic particles.

The presence of Fe oxides in waterbodies is due to: (1) dragging by water from soil or sediments bearing these minerals, either directly or through the air (see section 2.3.3), the nanometric size of Fe oxides facilitating their transport; (2) precipitation from dissolved Fe(II) or Fe(III) by effect of changes in pH, Eh, salt concentration or other chemical parameters. Also, microorganisms often catalyze a number of redox reactions (Konhauser *et al.*, 2011). (3) Transformation from precursors. Rejuvenation, maturation, aggregation and recrystallization reactions are common among Fe oxides, most of which are unstable.

Factors such as temperature, pH, Eh or the presence of foreign compounds (see section 2.2) play a key role in the dynamics of Fe oxides and affect the qualitative and quantitative composition of water as a result.

Acid mine drainage produced by sulfide microbial oxidation is a major source of water contamination worldwide. One striking example is provided by Rio Tinto in southwestern Spain (Fig. 6), a river where poorly crystalline Fe oxides such as schwertmannite, ferrihydrite and other crystalline phases resulting from their transformation (*e.g.* goethite) have been identified (Hudson-Edwards *et al.*, 1999; Perez-López *et al.*, 2011). As discussed below, the adsorption capacity of Fe oxides (especially the poorly crystalline phases) makes them effective carriers for trace elements, heavy metals and other toxic compounds in water.

Climate change is influenced by the Fe cycle because Fe carried by rivers or wind can reach the ocean and increase the Fe stock available to phytoplankton (Jickells *et al.*,



**Fig. 6.** Iron oxides in waters and sediments of Rio Tinto (SW Spain).

2005). Phytoplankton species take up carbon dioxide as they grow, thereby reducing the impact of greenhouse gases and global warming. Recent evidence indicates that the melting of free-floating icebergs is another Fe source for southern oceans (Raiswell *et al.*, 2008). Authigenic nanoparticles of schwertmannite, ferrihydrite and goethite formed during sulfide oxidation, and found in iceberg and subglacial sediments from Antarctica and Svalbard (Norway), might constitute an effective bioavailable Fe source by virtue of their high reactivity as suggested by TEM, SEM and chemical extraction data (Raiswell *et al.*, 2008).

Spectacular images of the ‘Blood Falls’ in the Taylor glacier (Antarctica) further testify to the ubiquity of Fe oxides. Under such extreme conditions, a plethora of micro-organisms catalyze the complex biogeochemical reactions which drive the formation of nanosized Fe oxides (Mikucki *et al.*, 2009).

### **2.3.3. Atmosphere**

Citizens in Sydney, Australia, woke up on 23 September 2009 to see a red–brown sky, and found that red dust had covered their gardens and birds had flown out of their nests. The event was so spectacular that many people suspected an apocalyptic Armageddon. A huge dust storm which had settled over the city and much of the state of New South Wales was carried east overnight by gale-force winds of up to 100 km/h. Besides quartz and other clay minerals such as kaolinite and illite, chemical and mineralogical analysis confirmed the presence of hematite as the main Fe oxide responsible for the red–brown colour (Radhi *et al.*, 2010). This was consistent with the origin of the aerosols: the Fe-rich, arid soils in central Australia. Less dramatically, dust-laden air masses

originating in the Sahara and Sahel deserts travel periodically over the Canary Islands and, either by dry deposition or washing out by rain, contribute a reddish mineral mixture to their soils. A combination of selective dissolution, magnetic methods and diffuse reflectance spectroscopy allowed Lázaro *et al.* (2008) to identify hematite, goethite and minor amounts of some ferrimagnetic iron oxides (maghemite and magnetite) in dust collected in Gran Canaria. One other, non-natural potential source of Fe oxides in the atmosphere is fly ash from industrial coal combustion and coal fires. Nanoscale hematite, magnetite and maghemite have been identified by TEM in such coal materials (Silva *et al.*, 2010, 2011). Of special note here is the fact that Fe oxides in clouds can be altered or rejuvenated by cycling with moisture-containing aerosols having a low pH owing to the presence of acid gases (Shi *et al.*, 2009). One example is the presence of carbonate-coated ferrihydrite, which can be released and become more bioavailable upon dissolution of the carbonate (Shi *et al.*, 2009). In all cases, Fe oxides have a substantial effect on the optical properties of the atmosphere, especially in the visible range, and hence on the Earth's radiative balance and climate (Sokolik & Toon, 1999).

The Fe oxides in dust falling on the ocean have substantial impact on Fe cycling and uptake by biota. In addition to soluble/labile Fe, nanoparticulate Fe oxides are seemingly incorporated by some phytoplankton species (Nodwell & Price, 2001). Surface blooms of *Trichodesmium* (a marine filamentous cyanobacterium that is very common in tropical oligotrophic oceans), which contribute significantly to biological fixation of atmospheric nitrogen, are triggered by the ability of this species to dissolve Fe oxides (ferrihydrite) coming from the atmosphere (Rubin *et al.*, 2011).

#### 2.3.4. Biosphere

Most Fe oxides, hematite excepted, are formed inside living organisms through a process called biomineralization. Like other biominerals, nanosized Fe oxides have homeostatic roles, are involved in the metabolism of Fe, act as navigation devices and can impart structural support, hardness and density to tooth structures (Frankel & Blakemore, 1991).

Ferrihydrite is the most widespread Fe oxide in living organisms. It occurs mainly as ferritin, a protein with a core of ferrihydrite 5–10 nm across that is found in all organisms from bacteria to plants (phytoferritin; Seckback, 1982) and humans (heart, spleen or liver). The protein coating, together with phosphate, prevents ferrihydrite from evolving towards a more crystalline Fe oxide (Reeves & Mann, 1991). Nanoparticles of goethite and lepidocrocite acting as teeth hardeners in the radula of some mollusca (*e.g.* limpets, chitons) allow them to graze algae growing on rocks (Lowenstam, 1981). Radula teeth include an outer layer of magnetite that is not in direct contact with the calcium phosphate tooth nucleus but isolated from it by a thin layer of lepidocrocite. Laboratory experiments suggest that such a singular distribution might be due to the presence of phosphate (Jurado *et al.*, 2003).

Biomagnetite in organisms has been described extensively in so-called “magnetotactic bacteria”, which have been found in lakes, sea (Blakemore, 1975) and anaerobic soils (Fassbinder *et al.*, 1990). These bacteria are capable of synthesizing chains of magnetite



crystals (<100 nm long) (Pósfai *et al.*, 2013) or other Fe minerals such as greigite ( $\text{Fe}_3\text{S}_4$ ), thereby allowing them to align and move parallel to the Earth's magnetic field lines (a phenomenon known as 'magnetotaxis'). Biogenic magnetite crystals can persist after the death of organisms and be deposited as magnetofossils, thus contributing to the magnetism of soils and sediments (Maher, 2011).

Magnetofossils were a key factor in the hot controversy about the existence of life on early Mars derived from the Martian meteorite ALH84001, probably the most extensively studied and discussed rock in the universe. The potential presence of fossil biogenic activity was based, among other evidence, on the presence of magnetite crystals similar in size and shape to those produced by terrestrial magnetotactic bacteria (McKay *et al.*, 1996). The initial paper, which is currently the most cited on Mars studies and highly ranked among those dealing with electron microscopy and Fe oxides, was followed by a large number of studies intended to confirm or refute the starting hypothesis. The main weapons deployed in this battle include backscattered scanning electron microscopy (Friedmann *et al.*, 2001) and, especially, conventional TEM and HRTEM, occasionally with the aid of tomographic, holographic and magnetic methods (Thomas-Keprta *et al.*, 2009; Buseck *et al.*, 2001, Pósfai *et al.*, 2013). The result has been an exhaustive analysis of the morphology and particle-size distribution of magnetite crystals.

On Earth, many other species capable of producing magnetite – such as migratory birds, homing pigeons, social insects (bees, termites and ants), butterflies, shellfish, turtle, salmon, trout, tuna, whales and humans – appear to use this mineral as a compass (Wiltschko & Wiltschko, 1995; Mann, 2001; Kirschvink *et al.*, 2001; Pósfai & Dunin-Borkowski, 2009). Imaging by TEM and diffraction methods showing the presence of magnetite nanoparticles in or around innervated structures in the tissues of these animals have provided a key tool for confirming the magnetite hypothesis. The abdomen of honeybees (Hsu *et al.*, 2007), the antennae of ants (de Oliveira *et al.*, 2010), the olfactory epithelium of the trout (Eder *et al.*, 2012) or the beak of homing pigeons (Fleissner *et al.*, 2003) are a few of the putative sites where bionanomagnetites have been detected. However, the magnetite-based magnetoreception mechanism is still under debate and has recently been questioned for homing pigeons (Treiber *et al.*, 2012).

Iron oxides such as ferrihydrite and magnetite can be formed extracellularly by various organisms such as *Gallionella ferruginea* or *Lepthotrix ochracea*, which play a major role in the oxidation of  $\text{Fe}^{\text{II}}$  under acid conditions or at Eh levels that are too low for abiotic oxidation (Fischer, 1988). One other intensively studied bacterium is *Thiobacillus ferrooxidans*, which operates in acid mine water by oxidizing  $\text{Fe}^{\text{II}}$  at a rate that is several orders of magnitude greater than that in inorganic systems (Fanning & Burch, 1997).

Iron oxide framboid clusters were found in biofilms of broken thigh bones from *Tyrannosaurus rex*. According to Kaye *et al.* (2008), recent bacterial contamination could be a more reasonable hypothesis than the more attractive one proposed by Schweitzer *et al.* (2005), who assigned the biofilms to ancient soft tissues preserved for tens of millions of years.

Microorganisms also play a major role in the dissolution of Fe oxides in soils. Thus, temporary soil saturation promotes microbial reduction and mobilizes poorly crystalline and crystalline Fe oxides as a result, thereby increasing Fe phytoavailability (Sánchez-Alcalá *et al.*, 2011). The forces of interaction between bacteria, typically in the micron-size range, and nanoparticles of Fe oxides have been measured quantitatively by atomic force microscopy *via* a technique known as “biological force microscopy” (Lower *et al.*, 2001) and operating in the nano-Newton range. Bose *et al.* (2009) found that dissimilatory bacteria can respire using hematite in anaerobic environments and that crystal size affects nanoparticle aggregation and hence particle–organism contact. Recently, Lu *et al.* (2012) reported a new mechanism for the mineral–bacteria interaction: a synergistic pathway by which the metabolism and growth of non-phototrophic bacteria can be stimulated by solar light through photocatalysis of natural Fe oxides acting as semiconducting minerals.

## 2.4. Does size matter in Fe oxides?

### 2.4.1. Colour

The bright, vivid colours of many soils (Fig. 7) are due to the pigmenting effect of Fe oxides. Colour-related terms such as ‘Mediterranean red soil’, ‘Terra Rossa’, ‘Rhodoxeralf’, ‘Krasnozem’ or ‘Latossolo Amarelo’ are common in many classification systems at different categorical levels, and thus recognize indirectly the key role of Fe oxides in soil properties. To the naked eye, goethite is yellow–brown, hematite usually red, lepidocrocite orange, ferrihydrite dark reddish brown, maghemite brown to brownish red and magnetite black (Cornell & Schwertmann, 2003).

Colour also depends on crystal size and shape. For example, the colour of hematite ranges from yellowish red for nanoparticles to purple for micrometer-sized samples or even black for large crystals (specularite) (Fig. 8). The mechanisms



Fig. 7. Iron oxides pigmenting different types of soils.

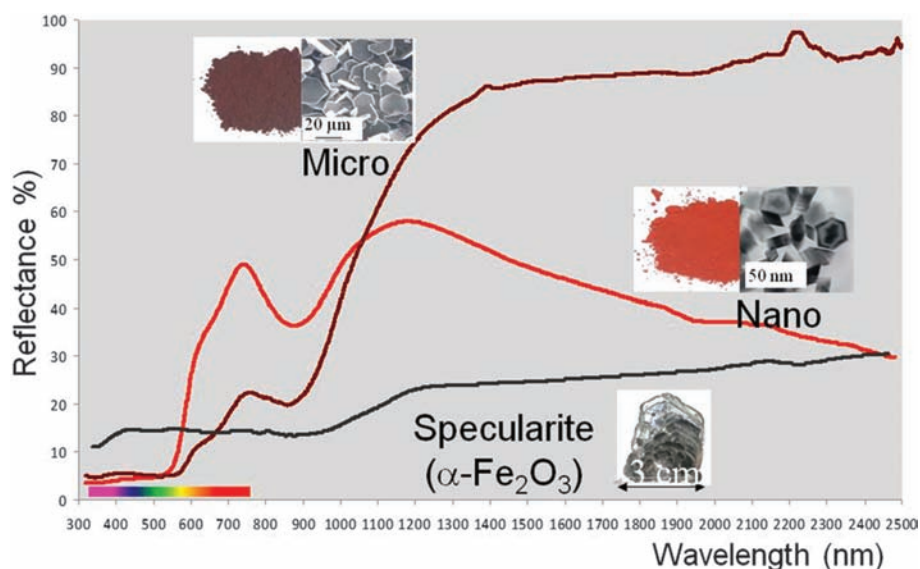


Fig. 8. Size effect on the diffuse reflectance and colour of hematite.

responsible for such colours are the scattering and absorption of light in the blue–green part of the visible spectrum which produces yellow and red hues. If absorption exceeds scattering over the entire visible range, then the Fe oxides are darker or even black as magnetite.

Besides visual comparison of mineral powder with Munsell charts (with chips ordered according to Hue, Value and Chroma), diffuse reflectance spectroscopy (DRS) is the most commonly used technique for studying colour in Fe oxides. Extensive use has been made of DRS to examine the effect of crystal size and shape, the presence of aluminium substitution or structural phosphorus in hematite or the sensitivity for quantifying minor amounts of different Fe oxides in soils and sediments, and also to elucidate the contribution of Fe oxides to soil genesis, aggregation and erosion, paleomagnetism and phosphate dynamics (Barrón & Torrent, 1984, 1986; Scheinost *et al.*, 1998; Torrent & Barrón, 2003, 2008; Fernandes *et al.*, 2004; Sellito *et al.*, 2009; Cañasveras *et al.*, 2010; Torrent *et al.*, 2010; Liu *et al.*, 2011).

#### 2.4.2. Magnetism

Iron oxides are very well known as the most important magnetic materials, *e.g.* in the industry of magnets, recording devices or inks and toners in photocopying machines. In these fields much research has been carried out on the effects of particle size and shape on the magnetic behaviour of Fe oxides (Cornell & Schwertmann, 2003).

The magnetism of rocks, sediments and soils is also due almost exclusively to Fe (and Ti-substituted) oxides, the characterization of which has been enabled by Mössbauer spectroscopy, neutron powder diffraction and magnetometric techniques.

Briefly, the most common Fe oxides can be classified as ferrimagnetic (magnetite, maghemite), weakly ferromagnetic (hematite) or antiferromagnetic (goethite and lepidocrocite) (Cornell & Schwertmann, 2003). The behaviour of ferrihydrite is more complex and can vary from speromagnetic for the amorphous phase (Coe & Readman, 1973) to ferrimagnetic for the most ordered and crystalline particles (Michel *et al.*, 2010).

Based on magnetic behaviour (magnetic susceptibility, saturation magnetization, remanence, coercivity) and decreasing particle size, ferrimagnetic minerals range from multidomain to pseudo-single domain, single domain and, finally, superparamagnetic for particles tens of nanometers in size. For example, magnetite and maghemite can exhibit magnetic susceptibility as much as four times higher in superparamagnetic crystals than in millimetric multidomain crystals (Peters & Dekkers, 2003). In the nanometric range, a peak in magnetic susceptibility and saturation magnetization can be observed at sizes near 10–15 nm (Maher, 1988; Morales *et al.*, 1999, Michel *et al.*, 2010). Magnetic parameters decrease below this size through the surface effect of spin canting. Therefore, materials science, archaeometry and paleomagnetic studies in geosciences (geophysics, geology and soil science), which have been used in recent years to elucidate the nature of palaeoclimates, require a good understanding of the effect of grain size on magnetic parameters. Thus, many models based on the paleorainfall and palaeotemperature relationships of various magnetic parameters require us to take into consideration not only the proportions of different Fe oxides but also their grain sizes (Jiang *et al.*, 2012; Torrent *et al.*, 2006; Liu *et al.*, 2010).

Magnetic susceptibility measurements on topsoils, which can be rapid and economical compared to other methods, have also been used to determine patterns of erosion and sedimentation in agricultural catchments (Royal, 2001) and, recently, to assess the potential of magnetites as sediment tracers for water erosion in Mediterranean soils (Guzmán *et al.*, 2010).

#### **2.4.3. Reactivity (stability, solubility, ion adsorption)**

The presence and abundance of Fe oxides in nature is influenced by their particle size. In fact, pioneering studies by Langmuir (1971) explained the equilibrium between goethite and hematite as a function of this factor. Recent thermodynamic studies of different Fe oxides have revealed the key role of crystal size (or surface area) and extent of hydration (Navrotsky *et al.*, 2008). Hematite becomes thermodynamically stable relative to goethite at surface areas below  $\sim 15 \text{ m}^2 \text{ g}^{-1}$  (*i.e.* at particle sizes around 60 nm if a spherical shape is assumed); however, no direct transformation from goethite to hematite has been observed under ambient conditions, so dissolution–reprecipitation is a more likely pathway for the conversion (Cornell & Schwertmann, 2003). Maghemite typically occurs naturally as a nanophase particle because an increase in particle size can lead to its transformation into hematite, which is the stable phase at crystal sizes  $> \sim 16 \text{ nm}$  (Navrotsky *et al.*, 2008). Similar thermodynamic constraints account for the impossibility of finding natural ferrihydrite or synthesizing it in crystal sizes  $> 10 \text{ nm}$  (Michel *et al.*, 2010).

The solubility of Fe oxides is a crucial property for predicting Fe bioavailability and understanding the iron cycle in nature. Although Fe oxides are highly insoluble [*e.g.* the

solubility product for  $[\text{Fe}][\text{OH}]^3$  is  $<10^{-38}$ ], there exist differences of a few orders of magnitude in this respect between oxide types. A modified version of the Kelvin equation relating the solubility of a material to its surface free energy and grain size predicts that, as grain size decreases, the solubility of particles will increase exponentially:

$$S/S_0 = \exp [(2\gamma V)/(RT_r)]$$

where  $S$  is the solubility of the material grains with an inscribed radius  $r$ ;  $S_0$  the solubility of the bulk material,  $\gamma$  its surface free energy,  $V$  the molar volume,  $R$  the gas constant and  $T$  the temperature. Based on this relationship, a poorly crystalline goethite with a crystal size of  $<10$  nm may well reach the solubility of ferrihydrite, the most soluble Fe oxide. The dissolution of Fe oxides in nature and in the laboratory *via* protonation, complexation or reduction also depends on crystal size and/or crystalline order (Schwertmann, 1991). This is why dilute, weakly acidic or complexing reagents capable of dissolving only the smaller Fe oxide particles in soils are the most successful chemicals for estimating Fe availability to plants. In particular, extraction with acid ammonium oxalate (Schwertmann, 1964), which essentially dissolves ferrihydrite and other poorly crystalline Fe oxides, is a good soil test for predicting Fe deficiency chlorosis in plants (del Campillo & Torrent, 1992a,b). Another good example of the effect of particle size on the siderophore-mediated dissolution of hematite was reported by Barton *et al.* (2012). Echigo *et al.* (2012, 2013) demonstrated how the nanopores in hematite, visualized using high-angle annular dark-field scanning transmission electron microscopy, are reactive sites for dissolution and enlarged by preferential etching.

Iron oxide surfaces exhibit high affinity for metals and anions (*e.g.* Zn, Cu, Cd,  $\text{PO}_4^{3-}$ ,  $\text{AsO}_4^{3-}$ ) and hence modulate the mobility of these species in various ecosystem compartments (biota, soils, rivers, lakes, oceans) (Cornell & Schwertmann, 2003; and references therein). Multiple studies have shown the strong dependence of sorption processes on particle size and hence on surface area. Not only surface area, but also surface charge can change with particle size and shape. In hematite and goethite, the surface hydroxyl configuration (SHC) governs the sorption of major sorbates such as phosphate. Theoretical and experimental studies on nanosized Fe oxides have shown SHC to depend on the relative development of crystal faces in variable hydroxyl densities and configurations (Barrón *et al.*, 1988; Torrent *et al.*, 1990; Colombo *et al.*, 1994; Barrón & Torrent, 1996). Papers by Madden *et al.* (2006) or Barton *et al.* (2011) also highlight how particle size matters for cation adsorption on crystalline nanohematite.

The transport of metals sorbed on Fe oxide nanoparticles is also of great environmental concern, especially in relation to acid mine drainage, industrial pollution and radioactive waste disposal (Hochella, 2002; Hochella *et al.*, 2008).

In addition to industrial applications (see next section), a number of natural and synthetic Fe oxides have found use in water purification; in fact, a substantial number of patents for Fe oxides rely on their ability to adsorb heavy metals, phosphate or arsenic. Iron oxide nanoparticles are also being assessed intensively for remediation of soils containing high levels of toxic metals (Mueller & Nowack, 2010).



Adsorption of organic compounds on Fe oxides has been studied extensively (Cornell & Schwertmann, 2003). In recent years, adsorption of dissolved organic (humic) matter in soils and sediment has become more relevant because of its impact on the carbon balance and hence on global warming. Based on recent research (Kaiser & Guggenberger, 2000; Lalonde *et al.*, 2012), Fe oxides provide an extremely efficient “rusty sink” for organic carbon and constitute a key factor in the long-term storage of organic carbon.

### 2.5. Selected old and new applications of iron oxides

From the first prehistoric paintings in caves [Altamira and El Castillo, 22,000 and 41,000 years ago, respectively (Pike *et al.*, 2012)] to the Pompeii brothel fresco (more than 1934 years ago) and today’s displays, natural and synthetic Fe oxides have conferred colour and beauty in the arts of painting, sculpture and architecture. It has also been suggested that the secret of not only the aesthetic beauty of some Stradivari violins, but also their heavenly sound, is in the varnish, which is dyed with a mixture of nanosized magnetite and hematite (Echard *et al.*, 2010). One of the best romantic writers, Johann Wolfgang von Goethe, after whom goethite was named, was keenly involved in studies of natural science and made one of the earliest contributions to the development of colour science in 1810.

Since the Iron Age (1200 BC), Fe oxides have been the main raw material for the iron and steel industry; their importance in the course of modern history is undeniable. For the past 100 years, the Haber process has been used to convert atmospheric nitrogen into ammonia, which is essential for manufacturing explosives and fertilizers. Haber’s discovery indeed changed the world in the past century: millions of people have died in armed conflicts, but at the same time, billions of people have been fed (Erisman *et al.*, 2008). One of the keys to the high efficiency of the process is that it uses a catalyst containing natural magnetite at extremely high pressures and high temperatures to break bonds in the nitrogen molecule which then combine with hydrogen to produce ammonia.

Nano-thermite, which is a vigorous, exothermic reaction between nano-hematite and aluminium powder reaching temperatures in the region of 2500°C, enough to melt metal Fe, is used for military purposes (propellants, explosives) or pyrotechnics. A recent “conspiracy theory” (Harrit *et al.*, 2009) based on optical microscopy, SEM, and X-ray energy dispersive spectroscopy analyses of some samples taken from the dust produced by the collapse of the World Trade Center speculates that the thermite reaction may have occurred in the catastrophe.

Finally, although Fe oxides have never been forgotten in history, lately we have been witnessing a real ‘come-back’. Tartaj *et al.* (2011, and references therein) summarized some of the “magic”, promising applications of nanosized Fe oxides as follows: (1) In the biomedical field. Nanomagnetites are used in contrast agents for Nuclear Magnetic Resonance Imaging, as carriers for selective drug delivery under a magnetic field and in hyperthermal treatments for cancer, where magnetite, stimulated by a magnetic field, can help locate heat sources in some target regions inside the human body. (2) In

energy-storage devices. The next generation of lithium ion batteries, which will be the key power supply for electronic devices and electric vehicles, might be based on hematite nanorods. (3) In catalytic reactions. In addition to the Haber process, magnetite is useful in major reactions exploiting the catalytic effect of Fe oxides (*e.g.* the Fenton reaction, which uses  $\text{H}_2\text{O}_2$  to oxidize contaminants, or the Fischer–Tropsch reaction, which is used to synthesize hydrocarbons from CO and  $\text{H}_2$ ). Magnetite and maghemite are currently being investigated extensively as magnetically recoverable nanocatalysts for a wide range of organic reactions with a view to developing more efficient, greener chemical processes (Polshettiwar *et al.*, 2011). Magnetite and hematite might be used as photocatalytic materials to generate  $\text{H}_2$  from water, just consuming solar energy, a more environmentally friendly power-production technology.

### 3. Manganese oxides

#### 3.1. Nanoscale nature

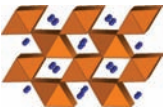
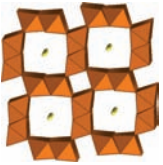
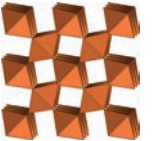
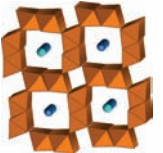

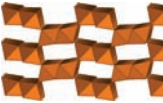
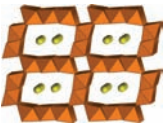
Most natural Mn oxides are nanosized and poorly crystalline, especially in soils and sediments (McKenzie, 1989; Dixon & White, 2002). This further complicates their positive identification with conventional techniques such as XRD because of their extensive dilution in these media. For instance, Mn oxides in soils are usually present at concentrations one or two orders of magnitude less than those of Fe oxides and clays, respectively. For this reason, much of the literature about this subject makes no distinction between Mn phases and typically uses the generic name “Mn oxides” for them. Positive identification of individual Mn phases is only possible in some concentrated forms such as coatings (mangans), veins or nodules. Selective dissolution (with hydroxylamine hydrochloride or the dithionite–citrate–bicarbonate mixture) has been used to detect them using differential XRD (Dixon & White, 2002). With powder X-ray and neutron diffraction, the Rietveld method provides good structure refinement. High-resolution imaging and electron diffraction have also been used as an essential supplement to elucidate many Mn oxide structures (Post, 1999).

Although >30 Mn oxides have been reported to date, only ~10 have been studied in detail (Table 4). In essence, Mn oxides can be classified structurally as follows:

##### 3.1.1. *Tectomanganates (tunnel Mn oxides)*

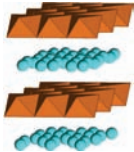
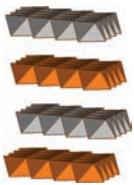

These consist of single, double or triple chains of edge-sharing  $\text{MnO}_6$  octahedra each formed by a nucleus of Mn surrounded by 6 O atoms, the chains sharing corners to form tunnel structures of square or rectangular cross-section. Manganite and pyrolusite (single chain) differ from hollandite, cryptomelane and ramsdellite (double chain), todorokite (triple chain) and romanechite (double and triple chain) in tunnel diameter and hence in surface area and accessibility for exchangeable ions. Intergrowth of hollandite and romanechite (Turner & Buseck, 1979), and the presence of variable tunnel widths in todorokite (Turner & Buseck, 1981) have also been reported. Several decades ago high-resolution TEM images and electron diffraction measurements confirmed the tunnel structure of these minerals (Fleischer & Richmond, 1943; Turner &

**Table 4.** Crystallographic data and structure for manganese oxides

Mineral	Formula	Crystal system	Unit-cell dimension (nm)			Structure
			<i>a</i>	<i>b</i>	<i>c</i>	
<i>Tunnel structures</i>						
Manganite	$\text{Mn}^{+3}\text{OOH}$	Monoclinic	0.530	0.528	0.531	
Hollandite	$\text{Ba}_x(\text{Mn}^{+4}\text{Mn}^{+3})_8\text{O}_{16}$	Monoclinic	1.001	0.288	0.972	
Pyrolusite	$\text{Mn}^{+4}\text{O}_2$	Tetragonal	0.440	0.440	0.287	
Cryptomelane	$\text{K}_x(\text{Mn}^{+4}\text{Mn}^{+3})_8\text{O}_{16}$	Monoclinic	0.994	0.287	0.971	
Todorokite	$(\text{Na,Ca,K})_{0.4}(\text{Mn}^{+4}\text{Mn}^{+3})_6\text{O}_{12} \cdot 3.5\text{H}_2\text{O}$	Monoclinic	0.976	0.284	0.957	
Ramsdellite	$\text{Mn}^{+4}\text{O}_2$	Orthorhombic	0.927	0.287	0.453	
Romanechite	$\text{Ba}_{0.66}(\text{Mn}^{+4}\text{Mn}^{+3})_5\text{O}_{10} \cdot 1.3\text{H}_2\text{O}$	Monoclinic	1.394	0.284	0.968	

(Continued)

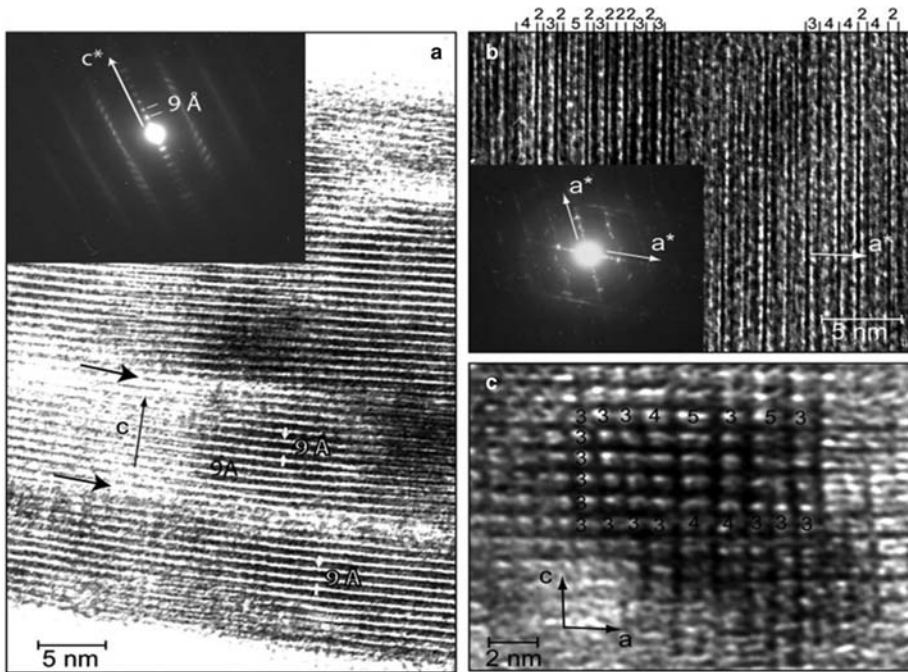
Table 4. Continued

Mineral	Formula	Crystal system	Unit-cell dimension (nm)			Structure
			<i>a</i>	<i>b</i>	<i>c</i>	
<i>Layer structures</i>						
Birnessite	(Na,Ca,Mn <sup>2+</sup> ) (Mn <sup>4+</sup> Mn <sup>3+</sup> ) <sub>7</sub> O <sub>14</sub> ·2.8H <sub>2</sub> O	Monoclinic	0.517	0.285	0.734	
Lithiophorite	LiAl <sub>2</sub> (Mn <sub>2</sub> <sup>4+</sup> Mn <sup>3+</sup> ) O <sub>6</sub> (OH) <sub>6</sub>	Trigonal	0.292		2.818	
Chalcophanite	Zn Mn <sub>3</sub> <sup>4+</sup> O <sub>7</sub> ·3H <sub>2</sub> O	Trigonal	0.753		2.079	

Buseck, 1981); other authors have also ‘visualized’ this kind of structure (Golden *et al.*, 1986; Shen *et al.*, 1993; Bodeř *et al.*, 2007; Fig. 9).

### 3.1.2. Phyllomanganates

Phyllomanaganates possess layered sheets of edge-sharing MnO<sub>6</sub> octahedral units. In birnessite, water and various cations (Na, Ca or Mn<sup>+2</sup>) are incorporated into the interlayer and affect the distance between sheets (Giovanoli & Arrhenius, 1988). Layers of (Li, Al)(OH)<sub>6</sub> octahedra are present in the interlayer region of octahedral Mn in lithiophorite and octahedral Zn alternating with water molecules that occupy interlayer positions present in chalcophanite. The structure of vernadite, an analogue of synthetic phase δ-MnO<sub>2</sub>, is still poorly known because of its poor crystallinity and it has been signalled as a variety of turbostratic birnessite (Manceau *et al.*, 1992; Villalobos *et al.*, 2006). In many cases, the analysis of lattice fringes and electron diffraction has been crucial for identifying Mn oxides (Chen *et al.*, 1986; Golden *et al.*, 1987; Van Tendeloo *et al.*, 2009). More recently, scanning tunnelling microscopy (STM), which reaches atomic scale, has been used to resolve the structure of some layered Mn oxides (Renner *et al.*, 2002).



**Fig. 9.** HRTEM images of a vernadite-todorokite particle from the outermost portion of a manganese concretion. (a) HRTEM image of a 1 nm-thick vernadite particle and electron diffraction (inset) showing the lattice fringe separation; (b) [001] zone-axis HRTEM image of a todorokite fibre, showing variable chain widths in the  $a$  direction, and chain dislocations in the  $b$  direction. The electron diffraction pattern (inset) has pronounced streaks along the two  $a^*$  directions; (c) [010] zone-axis HRTEM image showing coherent ( $c$  direction, vertical numbers) and incoherent ( $a$  direction, horizontal numbers) intergrowths of  $3 \times 3$ ,  $3 \times 4$  and  $3 \times 5$  tunnel structures (reproduced from Bodeř *et al.*, 2007, *Geochimica et Cosmochimica*, with the permission of Elsevier).

Most of the previous references and several reviews (McKenzie, 1989; Dixon & White, 2002) have reported TEM images of nanoscale Mn oxides in the form of needles (sometimes forming balls), flakes or plates of birnessite and lithiophorite.

### 3.2. Formation and occurrence

Manganese, the 12<sup>th</sup> most abundant element in the Earth's crust, appears in the early stages of magmatic crystallization in mafic rocks (*e.g.* basalt, gabbro), but also in many metamorphic and sedimentary rocks. Weathering of Mn(II)-bearing minerals releases  $\text{Mn}^{2+}$ ; this ion is easily oxidized and precipitated in the form of Mn oxides, which are the main players in the mineralogy and geochemistry of Mn in the upper crust (Post, 1999).

Extensive deposits of Mn oxides occur as nodules, micro-concretions, coatings and crusts at the bottom of the seas and oceans, covering  $\sim 10$ – $30\%$  of the deep Pacific floor (Crerar & Barnes, 1974; Menard & Shipek, 1958). Continental runoff and



hydrothermal/volcanic activity are thought to be the main sources for the formation of these deposits. Nodules, typically 0.5–25 cm in size, are brown–black and subspherical botryoidal in shape, bearing, together with Fe and Mn oxides, clay minerals, quartz, apatite, biotite and feldspars (Post, 1999). Birnessite, todorokite and vernadite are the major minerals identified so far (Burns & Burns, 1977). The structures of these phases have been difficult to decipher, but HRTEM observations have shown differences in the structure of todorokite from marine nodules compared to that of non-marine provenance (Turner *et al.*, 1982). HRTEM has also been a crucial tool for studying the presence of Fe–Mn oxides in deep sediments from the Red Sea (Taitel-Goldman *et al.*, 2009).

Mn oxides in nodules have a large adsorption capacity for heavy metals (Cu, Ni, Co); as a result, they govern the concentrations of these metals in seawater. Because they also contain substantial amounts other strategic metals, Mn nodules have commercial interest. Note that Mn oxides have been exploited as raw materials by the steel and alloy industries, and in the production of fertilizers, batteries, pigments, catalysts and water-purifying agents for many decades (Post, 1999).

Like Fe oxides, Mn oxides are ubiquitous in soils and sediments, where they occur as ped coatings (mangans), black varnish on pebbles, fine-grained aggregates, nodules and concretions (Dixon & White, 2002). Many textbooks assume that Mn oxide dendrites (Fig. 10) and other coatings consist mainly of pyrolusite but most deposits are in fact birnessite and/or romanechite (Post, 1999). Birnessite, vernadite, todorokite, hollandite and lithiophorite are by far the most common Mn minerals identified in soils (McKenzie, 1989; and references therein). According to Dixon & White (2002), birnessite occurs in young soils, todorokite in young and intermediate-age soils, and lithiophorite is relatively more abundant in old, strongly weathered soils.

Nodules or concretions ranging generally from 1 to 15 mm in size (Fig. 11) are common in soil horizons subject to seasonal waterlogging. In fact, the presence of these concretions is used as a diagnostic criterion for identifying fluctuations in the redox potential of soil. Observations with an electron microprobe (McKenzie, 1975)



**Fig. 10.** Manganese oxide dendrites on a calcarenite.

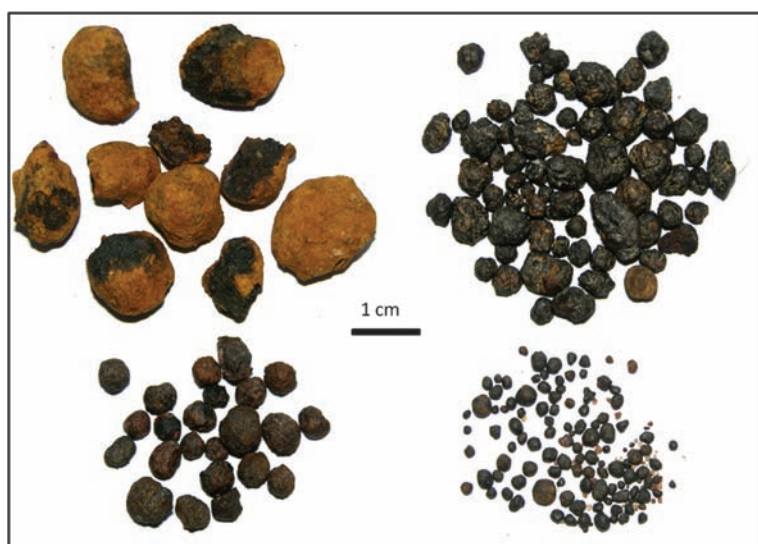


Fig. 11. Nodules from Spanish soil subject to seasonal waterlogging.

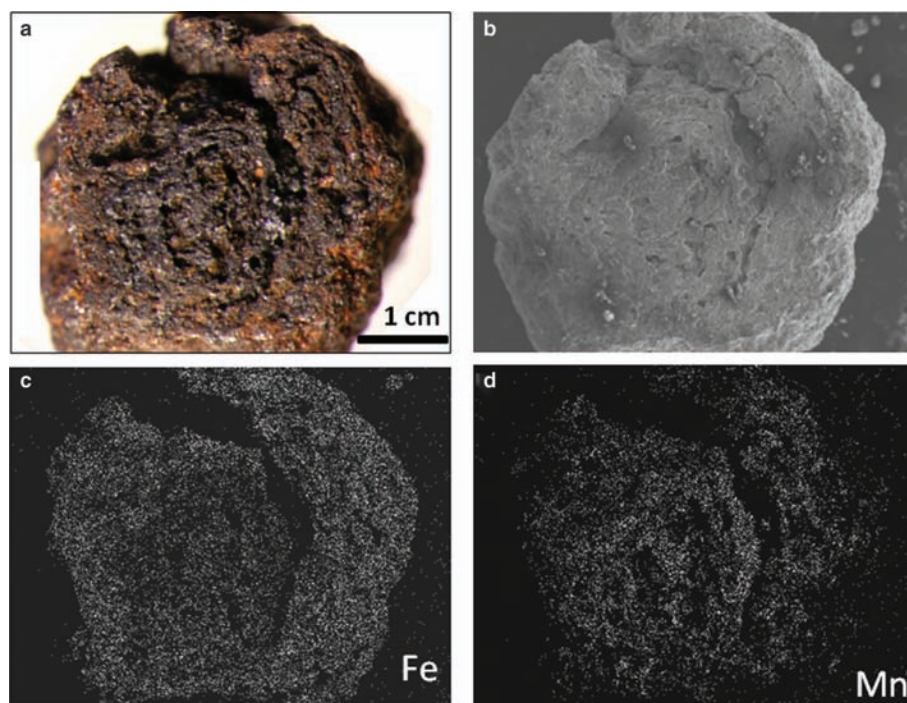
showed Mn accumulations to be invariably accompanied by high concentrations of Fe oxides (Fig. 12), mostly as ferrihydrite. Based on electron microscopy and synchrotron X-ray studies (Vodyanistkii, 2006, 2009), ferrihydrite and ferrioxhyte, together with vernadite and birnessite, were concentrated in the ferromanganic nuclei of nodules from Russian soils.

Microorganisms (particularly bacteria, fungi and algae) play a prominent role in the formation of most naturally occurring environmental Mn oxides. Enzymatic catalysis by phylogenetically diverse microorganisms has been found to accelerate Mn(II) oxidation and leads to the formation of biogenic Mn oxides (Tebo *et al.*, 2004). X-ray diffraction and absorption, and electron microscopy, have enabled the identification of mainly poorly crystalline layered-type Mn(IV) oxides (birnessite and vernadite) produced by *Pseudomonas putida* (Villalobos *et al.*, 2003, 2006). As with Fe oxides, preparing Mn oxides in the laboratory has improved our understanding of the major pathways for their formation in natural environments.

### 3.3. Environmental significance

Mn oxides are important constituents of soils and other environments for various reasons. First, Mn is an essential element for plant and animal nutrition. The crystallochemical and morphological properties of Mn oxides (size and shape, mainly) dictate Mn availability to plants. Also important in terms of plant performance are the effects of redox potential and pH on the availability and potential toxicity of Mn.

Second, manganese oxides are strong oxidants which can easily oxidize inorganic ions ( $\text{Co}^{+2}$  to  $\text{Co}^{+3}$ ,  $\text{Cr}^{+3}$  to  $\text{Cr}^{+6}$ , and  $\text{As}^{+3}$  to  $\text{As}^{+5}$ ) and organic molecules (*e.g.*



**Fig. 12.** (a) Section of a nodule from Fig. 11 with (b) SEM image, (c) Fe distribution, and (d) Mn distribution.

phenols and aromatic amines to polymeric products). Valence in Mn oxides varies widely. Only trivalent Mn is present in manganite; tetravalent Mn in pyrolusite, ramsdellite and chalcophanite; and a combination of tetravalent and trivalent Mn in hollandite, cryptomellane, todorokite, romanechite, lithiophorite and birnessite. The last mineral has also been found to contain some divalent Mn (Table 4). Internal valence changes in Mn oxides without release of  $\text{Mn}^{2+}$  make these minerals highly active as redox agents in soils (McBride, 1994). The redox range for the  $\text{Mn}^{4+}$  to  $\text{Mn}^{2+}$  reduction in soils and sediments falls above that for the  $\text{Fe}^{3+}$  to  $\text{Fe}^{2+}$  reaction, and occurs after the reduction of nitrate to nitrite. The reduction of sulfate to sulfide and methane formation occur below the redox ranges for Mn and Fe.

According to Sparks (1986), because Mn oxides can polymerize single organic compounds, soils may have been one of the cradles for the earliest organisms on Earth. The absence of  $\text{O}_2$  in the early atmosphere leads to an easily reducible substance, Mn oxide, which would have been able to accept electrons from a reduced environment until the eon, when  $\text{O}_2$  produced by photosynthesis was freed from water.

Third, Mn oxides have a large specific adsorption capacity for anions of weak acids (*e.g.* phosphate, molybdate, selenite) and weak hydrolyzed cations (*e.g.* Cu, Co, Ni, Pb, Zn). Previous evidence has been confirmed by electron microprobe analysis (McKenzie, 1975; Liu *et al.*, 2002). Because of their low point of zeta charge, high negative charge

and large surface area – most are poorly crystalline – Mn oxides exhibit strong specific adsorption (McKenzie, 1989). Therefore, they are important agents in the control of distribution and bioavailability of many essential and toxic elements such as heavy metals and radionuclides (Post, 1999). By virtue of their effect on the quality of marine waters, Mn oxides have been recognized as the scavengers of the environment (Goldberg, 1954; Hudson-Edwards, 2000). Mn oxides readily undergo cation exchange reactions showing, in some cases, exchange capacity above that of montmorillonite (Morgan & Stumm, 1965). Other studies on soils and stream sediments suggest that Mn oxides might serve as natural traps for heavy metals in contaminated mine waters (Lind & Hem, 1993; Prusty *et al.*, 1994). Analyses by TEM and energy dispersive X-ray (EDX) were essential for finding and characterizing ferrihydrite and a vernadite-like mineral associated with toxic metals in samples collected from the riverbeds and floodplains of the river draining the largest mining-contaminated site in the United States: the Clark Fork River Superfund Complex (Hochella *et al.*, 2005).

## 4. Aluminium oxides

### 4.1. Nanoscale nature and occurrence

Why, unlike iron, does aluminium (Al) metal not rust? Why does electrical current pass easily through two aluminium wires that are gently touching? Paradoxically, the key is the formation of a transparent, nanoscopic (2–4 nm) coating of Al oxide (poorly crystalline alumina,  $\text{Al}_2\text{O}_3$ ). In fact, aluminium is chemically more active than iron and quickly forms a hard, continuous coating that sticks tightly to the metal and protects its surface from further corrosion. By contrast, Fe oxide or rust flakes off and exposes iron surfaces to further corrosion. Regarding the second question, bulk alumina is an insulator, so no electric current should pass through the surface of two oxidized wires. However, because the alumina coating is very thin, typically of the same order of magnitude as the mean distance electrons can travel without undergoing energy loss (a few nanometers), it behaves as an efficient conductor, so the two wires maintain good electrical contact (Hochella, 2002).

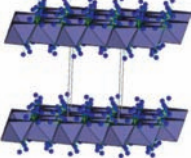

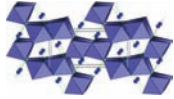
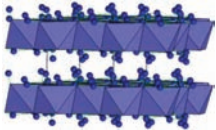
In natural environments, alumina, as the well crystallized mineral corundum, is present in igneous and metamorphic rocks, where it exhibits sizes well above the nanometer scale, fortunately, for the red and blue gem-quality corundum crystals known as ruby and sapphire.

A substantial proportion of the research on alumina is related to the Bayer process, which is the principal industrial procedure for producing this mineral, subsequently smelted to obtain aluminium, from bauxite, a sedimentary rock containing mainly gibbsite and boehmite. The Bayer process, which has changed very little since the first plant opened more than 100 years ago, produces more than 30 million tons of Al per year according to the International Aluminium Institute (<http://www.world-aluminium.org/Home>). An unfortunate ecological disaster occurred on October 4, 2010 at the Ajkai Timföldgyár alumina plant in Ajka (Hungary) that was shown extensively on TV.

A dam wall containing liquid wastes collapsed, releasing about a million cubic meters of what the press referred to as “toxic red mud”; the mud contaminated hundreds of hectares of farmland close to the Marcal river, a tributary to the Danube. The characteristic red colour was derived essentially from nanosized hematite (see section 2.4.1), which is the main pigment associated with Al oxyhydroxides (typically a white powder) in bauxites. The mud was strongly alkaline and contained titanium and vanadium compounds along with smaller amounts of other heavy metals, which were actually the toxic compounds. Due to its distinctive colour, the “wicked red hematite mud” helped to identify at a glance where contamination had occurred.

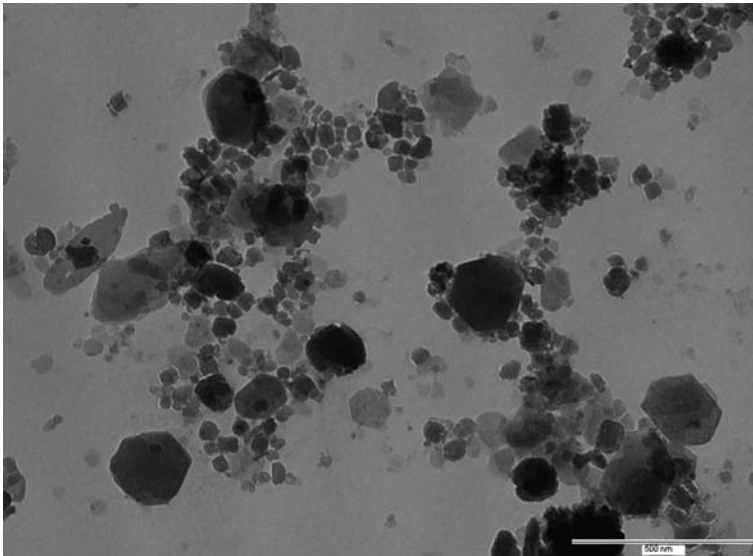
Gibbsite,  $\gamma\text{-Al(OH)}_3$ , is the principal constituent of bauxites in tropical regions and boehmite,  $\gamma\text{-AlOOH}$ , a major component of bauxites at Mediterranean sites (Wefers & Misra, 1987). Gibbsite and boehmite are present in appreciable amounts in soils (especially in tropical areas), whereas diaspore and bayerite occur only occasionally in them (Huang *et al.*, 2002). Consequently, most of the references to TEM or STM-AFM techniques applied to these Al oxides deal with gibbsite and boehmite (Table 5). The structure of gibbsite (also referred to in Europe as “hydrargillite”) consists of stacked  $\text{Al(OH)}_3$  sheets formed by octahedra sharing three edges, whereas that of boehmite, where half of the oxygen atoms are oxy-ions and the other hydroxyls, can be described as a double chain of  $\text{AlO}_6$  octahedra sharing six edges to form zigzagging

**Table 5.** Crystallographic data and structure for aluminum oxides.

Mineral	Formula	Crystal system	Unit-cell dimension (nm)			Structure
			a	b	c	
Gibbsite	$\gamma\text{-Al(OH)}_3$	Monoclinic	8.742	5.112	9.801	
Boehmite	$\gamma\text{-AlOOH}$	Orthorhombic	12.400	3.870	3.060	
Diaspore	$\alpha\text{-AlOOH}$	Orthorhombic	4.328	9.336	2.818	
Bayerite	$\alpha\text{-Al(OH)}_3$	Monoclinic	5.062	8.671	4.713	



layers held together by hydrogen bonds (Table 5). According to Eng *et al.* (2000) the structure of gibbsite can also be present in the surface of the hydrated  $\alpha$ - $\text{Al}_2\text{O}_3$  (corundum) changing its reactivity in comparison to that expected for the bulk mineral. Nanocrystalline boehmite is often referred to as ‘pseudoboehmite’ or ‘gelatinous boehmite’, and yields XRD patterns similar to boehmite but with broad peaks. Similar gelatinous aluminas in particle sizes of  $\sim 2$ – $3$  nm can also be obtained by a variety of chemical methods. The lack of a sufficient long-range crystalline order to obtain good XRD patterns hinders their accurate crystallochemical characterization and elucidation of which specific gelatinous Al alumina occurs in natural environments. However, weathering of Al-silicates is known to cause the release of  $\text{Al}^{3+}$  into slightly acidic soils solutions and natural waters, where it forms the hexaaqua ion,  $\text{Al}(\text{H}_2\text{O})_6^{3+}$ . This ion undergoes hydrolysis to a number of monomeric Al species that are important in soils because they are phytotoxic (Huang *et al.*, 2002). The monomeric species are quite reactive and dimerize and eventually form more complex, polymeric Al hydrolysis species. Hexameric ring or  $\text{Al}_{13}$  polynuclear species are among the proposed structures (Huang *et al.*, 2002). When these soluble polymeric species grow large enough, they eventually precipitate as a solid phase known as ‘gelatinous’ or ‘poorly crystalline Al hydroxide’. There are no unambiguous methods for identifying poorly crystalline Al hydroxides in soils, and only ammonium oxalate extraction, also used for poorly crystalline Fe oxides (see section 2.3.1), provides a rough estimate of their content in soils. Indeed, further research using TEM or HRTEM might help to better elucidate the complex world of the poorly crystalline Al oxyhydroxides. These gelatinous products are the precursors of more crystalline minerals (gibbsite or boehmite), the formation pathways of



*Fig. 13.* TEM image of gibbsite, together with hexagonal kaolinites in the clay fraction of a latosol.

which depend on a number of factors including temperature, pH, concentration and water activity. Studies based on synthetic models of different Al and Fe gels have helped improve our understanding of the effects of these factors (Colombo & Violante, 1996; Violante *et al.*, 1998).

Under the TEM, gibbsite, a well studied mineral in tropical soils, appears as relatively thick, roughly rectangular crystals 50–100 nm long (Fig. 13) (de Mesquita Filho & Torrent, 1993; de Brito Galvao & Schulze, 1996). Larger crystals appear as pseudo-hexagonal platy shapes or even elongated hexagonal rods. In volcanic soils (Andisols), gibbsite occurs as a product of the rapid weathering of volcanic ash (Allen & Hajek, 1989, Nieuwenhuysse & van Breemen, 1997).

Boehmite is much less abundant in soils than is gibbsite. The former has been identified in strongly weathered soils (Gilkes *et al.*, 1973), where it appears as aggregated tabular particles similar to those of its synthetic counterpart (Moreaud *et al.*, 2009).

#### 4.2. Environmental significance

Most of the effects of Al oxides in soils and other environments are shared with Fe oxides. Both have a significant influence on the formation of stable soil aggregates which help to improve the permeability of soil and reduce its erodibility. Aggregates stabilize by establishing direct linkages with phyllosilicates or interacting with organic compounds. In turn, organic matter can inhibit the crystallization of Al hydroxides and stabilize them as a poorly crystalline phase (Huang & Violante, 1986). Aluminium and iron oxides may even cement soils and form plinthic or lateritic horizons, which are very common in tropical soils. By using HRTEM, Jones & Uehara (1973) succeeded in confirming the presence of a poorly crystalline (gelatinous alumina) linkage between clay particles in Hawaiian soils.

Similarly to Fe oxides (see Section 2.4.3), Al oxides influence the turnover of soil organic C through retention on their surfaces. This effect is especially obvious in allophanic soils (Wada, 1995). Many Oxisols from tropical regions have limited losses of C, and hence also limited CO<sub>2</sub> emissions, by effect of their containing Al oxides (Huang *et al.*, 2002).

Phosphorus, an essential, limiting nutrient in terrestrial and aquatic ecosystems, has a very strong affinity for Al and Fe oxides (Parfitt, 1978). Phosphate can be adsorbed or occluded on Al oxides, which decreases its bioavailability. In turn, organic matter competes for P sorption sites and affects the dynamics of this nutrient (Afif *et al.*, 1995). Aluminium oxides can also adsorb alkaline cations (Ca, Mg, Ba) and heavy metals (Cu, Cd, Zn, Mn, Cr, Hg, As) in a specific manner (Goldberg *et al.*, 1996), which testifies to their unquestionable environmental role.

### Acknowledgments

This review was partly supported by the Spain's Ministerio de Educación y Ciencia, Project CGL 2010-15067, and the European Regional Development Fund. P.A.